THE JOURNAL OF BIOLOGICAL CHEMISTRY VOL. 281, NO. 6, pp. 3505–3512, February 10, 2006

Apical Transport and Folding of Prostate-specific Membrane Antigen Occurs Independent of Glycan Processing*

Received for publication, August 26, 2005, and in revised form, October 7, 2005 Published, JBC Papers in Press, October 12, 2005, DOI 10.1074/jbc.M509460200

Deborah Castelletti[‡], Giulio Fracasso[§], Marwan Alfalah[‡], Sara Cingarlini[§], Marco Colombatti[§], and Hassan Y. Naim[‡1]

From the [‡]Department of Physiological Chemistry, University of Veterinary Medicine Hannover, Bünteweg 17, D-30559 Hannover, Germany and the [§]Department of Pathology, University of Verona, I-37100 Verona, Italy

Prostate-specific membrane antigen (PSMA) is an integral cell-surface membrane glycoprotein that is overexpressed in prostate carcinomas rendering it an appropriate target for antibody-based therapeutic strategies. The biosynthesis of PSMA in transfected COS-1 cells reveals a slow conversion of mannose-rich to complex glycosylated PSMA compatible with slow transport kinetics from the endoplasmic reticulum to the Golgi. Importantly, mannose-rich PSMA persists as a trypsin-sensitive protein throughout its entire life cycle, and only Golgi-located PSMA glycoforms acquire trypsin resistance. This resistance, used here as a tool to examine correct folding, does not depend on the type of glycosylation, because different PSMA glycoforms generated in the presence of inhibitors of carbohydrate processing in the Golgi are also trypsin resistant. The conformational transition of PSMA to a correctly folded molecule is likely to occur in the Golgi and does not implicate ER molecular chaperones, such as BiP. We show here that PSMA is not only heavily *N*- but also *O*-glycosylated. The question arising is whether glycans, which do not play a role in folding of PSMA, are implicated in its transport to the cell surface. Neither the cell-surface expression of PSMA nor its efficient apical sorting in polarized Madin-Darby canine kidney cells are influenced by modulators of *N*- and *O*-glycosylation. The acquisition of folding determinants in the Golgi, therefore, is an essential prerequisite for protein trafficking and sorting of PSMA and suggests that altered or aberrant glycosylation often occurring during tumorigenesis has no regulatory effect on the cell-surface expression of PSMA.

Prostate cancer is one of the most common malignancies diagnosed in men and represents a significant worldwide health problem. No conventional treatment is effective following relapse or in case of metastatic disease. In fact, in nearly all of the patients relapsing, cancer progresses despite initial treatment even with the most updated forms of therapy. Biomarkers of prostate cancer have become available recently for the diagnosis, immunotherapy, and predicting of disease progression of prostate cancer (1). In particular, the prostate specific membrane antigen (PSMA)[2] represents a suitable cell-surface marker that is being considered in the management of prostate cancer (2). PSMA is an integral membrane glycoprotein of 110 kDa, found initially in LNCaP cells by immunoprecipitation (3). The analysis of *in vivo* distribution and the biological function of PSMA led to identify the protein not only in prostate (4, 5) but also in several other tissues, where PSMA acts as a glutamate carboxypeptidase on different alternative substrates (6, 7). Although the function of PSMA in prostate has not been clarified yet, its expression is enhanced in higher grade cancers, metastatic disease, and hormone-refractory prostate carcinomas (8, 9). Moreover, PSMA is present at the surface of endothelial cells found in tumors of different histotype but absent from normal endothelial cells (10). Radioimmunoconjugates of anti-PSMA monoclonal antibodies (mAbs) are currently used as imaging agents for prostate cancer (11). Moreover, it has been observed that, following contact with antibodies, PSMA is rapidly and efficiently internalized by the target cell and localizes in a juxtanuclear region of the cell (12). PSMA represents therefore a very attractive marker for passive immunotherapy with mAbs or their armed derivatives (13). Indeed, results obtained in our laboratory demonstrated that PSMA-positive cells are intoxicated by anti-PSMA antibody linked to the ricin toxin A-chain with high efficiency (14). Most types of immunotoxins need to be internalized and transported through intracellular compartments before exerting their cytotoxic effect. This requires that a complex series of phenomena take place in an orderly fashion in appropriate locations within the cell. These events in turn are likely to be influenced by the properties and physiology of the relevant target molecules. The enzymatic activity of PSMA and presumably also its folding and antibody recognition may be influenced by a differential glycosylation in tumor or normal cells (15). The optimization of the overall cytocidal potential of immunotoxins requires therefore elucidation of the properties and physiology of PSMA in cells. In particular, phenomena like rate of translation, maturation during biosynthesis, association with membrane microdomains, cell-surface expression, internalization, and turnover all may have important consequences on the sensitivity of prostate tumor and normal cells to treatment with immunotoxins.

Similar to many other type II transmembrane proteins, PSMA is highly glycosylated (16). In particular, PSMA has ten potential *N*-glycosylation sites. At least nine of them, located in the PSMA ectodomain, are indeed modified by carbohydrates that contribute to the 20–25% of the molecular weight of the native PSMA. As expected, a severe impairment of glycosylation, induced for instance by treatments with tunicamycin, causes the generation of an enzymatically inactive protein that is retained intracellularly (16, 17). This is likely to be due to misfolding or inhibition of dimerization, which are crucial for the generation of an active protein (18).

In the present study we report first on the biosynthesis, processing, and transport of PSMA in transfected COS-1 cells, where PSMA is expressed as a complex glycosylated protein on the cell surface, similar to PSMA molecules found in tumor tissues or serum (15). The possible role of glycans on the trafficking of PSMA toward the cell surface was

* This work was supported by the Deutsche Forschungsgemeinschaft (Bonn, Germany, Grant Na 331/1-4 to H. Y. N.) and by MIUR (PRIN 2003) and from Fondazione Cassa di Risparmio di Verona, Vicenza, Belluno e Ancona, Bando 2004 Integrazione Tra Tecnologia e Sviluppo di Settore (to M. C.). The costs of publication of this article were defrayed in part by the payment of page charges. This article must therefore be hereby marked "*advertisement*" in accordance with 18 U.S.C. Section 1734 solely to indicate this fact.

[1] To whom correspondence should be addressed. Tel.: 49-511-953-8780; Fax: 49-511-953-8585; E-mail: hassan.naim@tiho-hannover.de.

[2] The abbreviations used are: PSMA, prostate-specific membrane antigen; hPMSA, human PMSA; DMEM, Dulbecco's modified Eagle's medium; dMM, deoxymannojirimycin; Endo F, endo-β-*N*-acetylglucosaminidase F; Endo H, endo-β-*N*-acetylglucosaminidase H; mAb, monoclonal antibody; ER, endoplasmic reticulum; TX-100, Triton-X 100; TEMED, *N*,*N*,*N*′,*N*′-tetramethylethylenediamine; PBS, phosphate-buffered saline; ELISA, enzyme-linked immunosorbent assay; MDCK, Madin-Darby canine kidney cell.

investigated by using specific inhibitors of *O*- and *N*-glycosylation. A similar experimental approach was also used in polarized MDCK cells to determine whether or not apical sorting signals of PSMA are located in its *O*- and *N*-glycans. Furthermore, the folding status of PSMA in the early biosynthetic stages and in particular its association with typical ER-resident chaperones were examined.

EXPERIMENTAL PROCEDURES

Materials and Reagents—Tissue culture dishes were obtained from Greiner (Hamburg, Germany). Streptomycin, penicillin, glutamine, Dulbecco's modified Eagle's medium (DMEM), and methionine-free DMEM were purchased from Invitrogen. Fetal calf serum, pepstatin, leupeptin, aprotinin, trypsin inhibitor, molecular mass standards for SDS-PAGE, biotin-*N*-hydroxysuccinimide ester (Biotin-NHS), streptavidin horseradish peroxidase, inhibitors of specific *N*-glycosylation reactions (deoxymannojirimycin, swainsonine, and monensin), and an inhibitor of *O*-glycosylation, benzyl-*N*-acetylgalactosamine (benzyl-GalNAc) were purchased from Sigma (Deisenhofen, Germany). Phenylmethylsulfonyl fluoride, antipain, and soybean trypsin inhibitor were purchased from Roche Diagnostics (Mannheim). L-[^{35}S]Methionine (>1000 Ci/mmol) and protein A-Sepharose were obtained from Amersham Biosciences (Freiberg, Germany). Acrylamide, *N,N′*-methylenebisacrylamide, and TEMED were purchased from Carl Roth GmbH (Karlsruhe, Germany). SDS, ammonium persulfate, dithiothreitol, and Triton X-100 (TX-100) were obtained from Merck, (Darmstadt, Germany). Endo-β-acetylglucosaminidase H (Endo H) and endo-β-*N*-acetylglucosaminidase F-glycosidase (Endo F) were purchased from PerkinElmer Life Sciences. Trypsin and chymotrypsin were purchased from Sigma-Aldrich. The anti-PSMA mAb J591, described by H. Liu *et al.* (12), was kindly supplied by Dr. N. H. Bander (Medical College of Cornell University, New York). The murine 7E11c mAb (3), recognizing the cytosolic tail of PSMA, was purified from the supernatant of the hybridoma HB-10494 (American Type Culture Collection, Rockville Pike, MD) according to standard chromatographic methods. The anti-sucrase-isomaltase antibodies, mGlu1, mGlu2, and mGlu3, were a generous gift of Dr. D. Swallow (The Galton Laboratory, University College London, UK). The anti-BiP and anti-calnexin antibodies were purchased from Stressgen (Victoria, Canada). The anti-rabbit peroxidase-conjugated secondary antibody and the Hybond-P polyvinylidene difluoride membranes were obtained from Amersham Biosciences. The SuperSignal® ELISA Fempto Maximum Sensitivity Substrate kit was from Pierce, and Kodak BioMax XAR films were from Sigma-Aldrich.

Cloning of Human PSMA—A cDNA encoding the human PSMA (hPSMA) was cloned from LNCaP cells using as a template the mRNA purified from LNCaP cells. The following primers were designed based on the nucleotide sequence reported by R. S. Israeli *et al.* (5) and used to obtain two PSMA fragments of 1471 bp and 1426 bp in length, respectively. The primers TGCAGGGCTGATAAGCGAG and AGCCACGCCACGCTCTTG were used to generate a fragment spanning the 5′-region of PSMA that was subcloned into the pBS vector (Invitrogen) in correspondence of a SmaI and a EcoRI restriction enzyme sites. Two other oligonucleotides (the forward primer TCATCCAATTGGATACTATG and the reverse primer TCTTTCTGAGTGACATAC) enabled to amplify a second PCR product that was cloned into the same vector (between EcoRV and EcoRI restriction enzyme sites) and overlapped with the first fragment of PSMA. The complete cDNA sequence of PSMA was finally digested with BamHI and XhoI enzymes and subcloned into the pcDNA3.1 vector (Invitrogen) to obtain the pcDNA 3.1-hPSMA construct.

Transient Transfection of COS-1 Cells, Biosynthetic Labeling, Immunoprecipitation of Total Cellular Extracts, and Western Blotting—COS-1 cells were cultured in 10-cm Petri dishes and in DMEM supplemented with 10% fetal bovine serum and 2 mM L-glutamine. When the cells reached a confluence of ~30–40%, they were transiently transfected with 5 μg of pcDNA 3.1-hPSMA. The transfection was carried out according to the DEAE-dextran-based method described previously (19). Briefly, cells were incubated in the presence of DNA and DEAD-dextran for 1 h at the standard culturing conditions and then left for further 3 h in the complete DMEM supplemented with 1 μg/ml chloroquine. After washings, the cells were biosynthetically labeled with 100 μCi of [^{35}S]methionine for different time intervals, according to the experimental protocol. In pulse-chase experiments, the cells were pulsed for 30 min and then incubated for further 30 min, 1, 1.5, 2, 4, or 6 h at 37 °C in the presence of fresh medium containing cold methionine.

The cells were solubilized on ice for 1 h by using a combination of 0.5% TX-100 and 0.5% sodium deoxycholate, dissolved in PBS, supplemented with a mixture of protease inhibitors (1 mM phenylmethylsulfonyl fluoride, 1 μg/ml pepstatin, 5 μg/ml leupeptin, 5 μg/ml aprotinin, 1 μg/ml antipain, and 50 μg/ml trypsin inhibitor). After removal of cell debris by centrifugation and pre-clearing of the total extract with protein A-Sepharose (as described in more detail in Ref. 20), the supernatant was immunoprecipitated with a combination of the J591 and 7E11c anti-PSMA mAb. In some experiments immunoprecipitation with each individual antibody, *i.e.* 7E11c or J591, was performed. Solubilization of cells was also performed under denaturing conditions. Here, the cells were treated for 10 min at room temperature with 0.1% SDS in PBS and the mixture of protease inhibitors. TX-100 was then added to the extracts at a final concentration of 1% to obtain a 10-fold concentration of TX-100 *versus* SDS. Immunoprecipitation was then carried out using the 7E11c antibody. Antigen-antibody complexes were recovered by using 30 μl of protein A-Sepharose beads and then eluted by boiling in 1% SDS and processed by SDS-PAGE on 7% polyacrylamide gels. Proteins were finally detected by exposure of the gel to a Kodak X-Omat AR film and autoradiography (using a PhosphorImager purchased by Bio-Rad).

When required, immunoprecipitated proteins were subjected to enzymatic digestion with either Endo H or with Endo F according to a method described previously (21). Furthermore, the effect of proteases on PSMA immunoprecipitated in its native form was investigated. After washings, the protein A-Sepharose beads binding the immunocomplexes were resuspended in 25 μl of 0.1% TX-100/PBS containing different amounts of either trypsin or chymotrypsin (see "Results") and 10 μg of bovine serum albumin, used as a carrier. The reaction was prolonged for 30 min at 37 °C and blocked by boiling the samples at 95 °C in the presence of additional 25 μl of Laemmli-containing reducing buffer. The intensity of the protein bands obtained by autoradiography was then quantified by using the Quantity One software (Bio-Rad).

Western blot analysis was also performed using total lysates from COS-1 cells that were transfected with pcDNA 3.1-hPSMA. Here, 50 μg cellular proteins were used. The antibody 7E11c was used for antigenic detection. This antibody recognizes denatured forms of both the mannose-rich and complex glycosylated form of PSMA (see "Results").

Co-immunoprecipitation with BiP and Calnexin—To assess the possible interaction of PSMA with BiP or calnexin, total cellular extracts from four plates of transiently transfected COS-1 cells were immunoprecipitated with either anti-BiP or anti-calnexin mAb (22). To study the interaction with BiP, pulse-chase experiments were performed by chasing the cells for 30 min, 1, 2, 4, or 6 h after 30-min labeling with [^{35}S]methionine. After the indicated time intervals, the cells were washed with cold PBS and lysed in a

buffer containing 1% TX-100 and supplemented with a mixture of protease inhibitors (see above) and 10 μg of apyrase (Sigma). When a possible interaction with calnexin was assayed, cells were pulsed for 1 h at 37 °C and chased for 4 h either at 37 °C or at 15 °C. Immunoprecipitated proteins were eluted from protein A-Sepharose by boiling for 5 min at 95 °C in the presence of 1% SDS. Following dilution with 1% TX-100, samples were further processed to detect PSMA with J591 and 7E11c. Protein fractions depleted from BiP or calnexin were separately immunoprecipitated to detect non-interacting PSMA molecules. The possible interaction of PSMA and sucrase-isomaltase with these chaperones was investigated also by Western blotting, after immunoprecipitation of PSMA or sucrase-isomaltase from transiently transfected COS-1 cells. Human sucrase-isomaltase, expressed using the pSG8-hSI-vector (23), was immunoprecipitated with a combination of mAbs mGlu1, mGlu2, and mGlu3. Proteins were subjected to SDS-PAGE on 7% polyacrylamide gels and blotted onto a polyvinylidene difluoride membrane according to manufacturers' instructions. Anti-BiP and anti-calnexin antibodies were added to the membranes followed by anti-rabbit peroxidase-conjugated secondary antibodies. The antigenic detection in a chemiluminescent reaction employed the SuperSignal® ELISA Fempto Maximum Sensitivity Substrate kit.

Cell-surface Immunoprecipitation from COS-1 Cells—COS-1 cells were transfected and labeled following the same procedure described above. Two days post-transfection, cells were labeled for 6 h, and surface-expressed PSMA molecules were immunoprecipitated from intact cells by using the mAb J591. Unbound antibodies were removed by washing the cells three times with cold PBS and were further subtracted by using a cold-lysate of COS-1 cells transfected with PSMA. Cells were lysed for 1 h at 4 °C, and the antigen-antibody complexes from the cell surface were recovered with the addition of protein A-Sepharose. Intracellular PSMA was then immunoprecipitated from the supernatant by J591 and 7E11c mAb used in combination.

To test the role of inhibitors on the maturation process of membrane proteins, inhibitors of the glycosylation were separately added to the medium during the preincubation of transfected COS-1 cells in methionine-free medium as well as during the labeling with [^{35}S]methionine. Benzyl-GalNAc was used as an inhibitor of the *O*-glycosylation at 4 mM final concentration, whereas the following inhibitors of the *N*-glycosylation process were considered: deoxymannojirimycin (dMM), which inhibits the *cis*-Golgi mannosidase I, and swainsonine and monensin, active in the *medial*-Golgi and the *trans*-Golgi, respectively. dMM was used at 5 mM, whereas swainsonine and monensin were given to cells at 4 μg/μl and 1 μM final concentrations, respectively.

Detection of Cell-surface Antigens by Biotinylation—COS-1 cells were transfected with pcDNA 3.1-hPSMA as described above and incubated 2 h post-transfection with the glycosylation inhibitors dMM (5 mM), swainsonine (4 μg/μl), benzyl-GalNAc (4 mM), or without the inhibitors. The media were changed three times during a period of 48 h, and fresh glycosylation inhibitors were added at the same concentrations. Thereafter, the cells were washed twice with ice-cold PBS to remove amine-containing culture media and cellular proteins. Biotin-NHS in PBS at 1 μg/ml was added to the cells and left on ice for 30 min. The cells were then washed twice with ice-cold PBS, quenched with 100 mM glycine, and solubilized as described above. Immunoprecipitation with anti-PSMA antibodies (J591/7E11c) was performed, and the immunoprecipitates were subjected to Western blot analysis. The chemiluminescent detection of PSMA was carried out using streptavidin horseradish peroxidase and the SuperSignal® ELISA Fempto Maximum Sensitivity Substrate kit.

Indirect Immunofluorescence—Subcellular localization of PSMA in transfected COS-1 cells in the presence or absence of glycosylation inhibitors was performed using indirect immunofluorescence. Here, the transfected cells were incubated on coverslips with or without the glycosylation inhibitors dMM, swainsonine, and benzyl-GalNAc using similar procedure as described above. The cells were fixed with 4% paraformaldehyde and permeabilized with 0.5% saponin to visualize intracellular PSMA. The cell-surface localization was analyzed in non-permeabilized cells. Immunolabeling was carried out using anti-PSMA antibodies (combination of J591 and 7E11c) at 1:100 dilution. The secondary antibody was rabbit anti-mouse conjugated to Alex Fluor 488. The fluorescence images were visualized using a Leica TCS SP2 confocal laser microscope with a 63× water planapochromat lens (Leica Microsystems).

Generation of MDCK Stable Cell Lines Expressing hPSMA and Cell-surface Immunoprecipitation—Stable MDCK cells expressing hPSMA were obtained by using an Eppendorf microinjector (FemtoJet Eppendorf, Hamburg, Germany). Selection of cells containing pcDNA 3.1-hPSMA were positively selected by adding neomycin (500 μg/ml) to the DMEM medium. PSMA expression was finally confirmed by immunoprecipitation (see above).

To immunoprecipitate selectively PSMA molecules from the apical or from the basolateral surface of polarized MDCK, cells were cultured to complete confluence on transmembrane filters (24). During the preincubation with methionine-free medium and the 4-h pulse, cells were treated either with 5 mM dMM or with 4 mM benzyl-GalNAc, as inhibitors of the *N*- and the *O*-glycosylation, respectively. The J591 anti-PSMA mAb was used to immunoprecipitate PSMA from both the apical and the basolateral surface of MDCK cells, whereas a combination of both J591 and 7E11c mAb precipitated intracellular PSMA molecules.

RESULTS

Biosynthesis and Glycosylation of PSMA—COS-1 cells were transiently transfected with a cDNA encoding human PSMA (pcDNA 3.1-hPSMA) and biosynthetically labeled with [^{35}S]methionine for 4 h. After solubilization with a combination of TX-100 and sodium deoxycholate, PSMA was immunoprecipitated from the cell lysates by using a combination of two anti-PSMA mAb, J591 and 7E11c. Preliminary experiments elucidated that mAb J591, directed against a luminal epitope of PSMA, immunoprecipitated both the immature precursor and the complex glycosylated form (of ~100 and 110 kDa, respectively) with comparable efficiency, whereas 7E11c, recognizing the cytosolic tail, preferentially binds to the immature protein. The immature and the mature forms were discriminated based on their sensitivity to treatment with Endo H (Fig. 1). Endo H digests mannose-rich *N*-linked glycans, whereas complex carbohydrates are resistant to this enzyme. The substantial shift in the size of the lower 100-kDa band upon Endo H treatment confirmed that this band corresponds to the ER-localized precursor of PSMA. To gather information on the trafficking rate of PSMA between the ER and the Golgi and the kinetics of the glycosylation event, transfected COS-1 cells were labeled with [^{35}S]methionine for 30 min followed by several chase times (Fig. 1). 1 h into the chase, the biosynthetic forms of PSMA comprised a major mannose-rich form and a faint protein band that has acquired a substantial Endo H-resistance indicative of complex glycosylation and maturation. The half-life for the conversion of mannose-rich PSMA to a complex glycosylated species was ~120 min (Fig. 1*B*). After 4 and 6 h the proportion of the mature protein progressively increased. The persistence of major proportions of PSMA as a mannose-rich glycosylated polypeptide after 6 h of chase supports the notion that the transport rates of PSMA are very slow.

Implication of N- and O-Glycosylation in the Transport and Cell-surface Expression of PSMA—Altered and aberrant glycosylation has been described to occur in essentially all types of experimental and

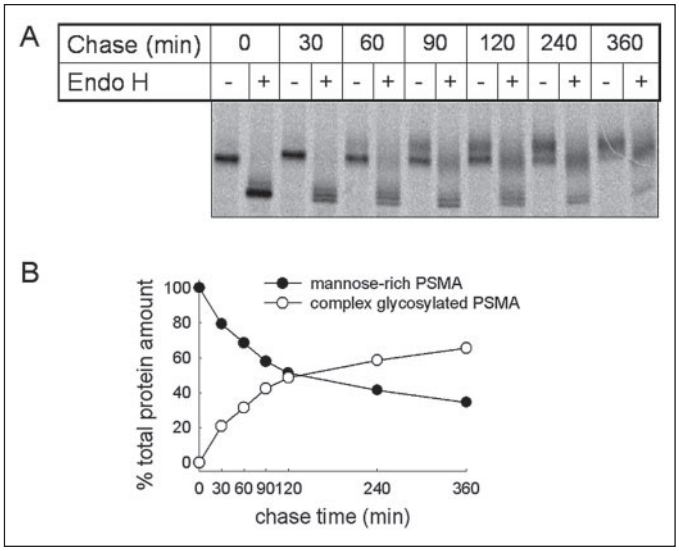

FIGURE 1. **PSMA is slowly transported in transfected COS-1 cells.** *A*, COS-1 cells, transiently transfected with the hPSMA-pcDNA 3.1 vector, were biosynthetically labeled for 30 min at 37 °C and chased for the indicated time intervals. After immunoprecipitation using a combination of the J591 and 7E11c anti-PSMA mAb, proteins were either treated with Endo H or left untreated and then analyzed by SDS-PAGE and autoradiography. *B*, quantification of the pulse-chase experiment shown in *A*. The proportions of mannose-rich PSMA (*filled circles*) and of complex glycosylated PSMA (*empty circles*) were calculated as percentages of total immunoprecipitated PSMA. The point of intersection represents the half-life for the conversion of mannose-rich PSMA to the complex form.

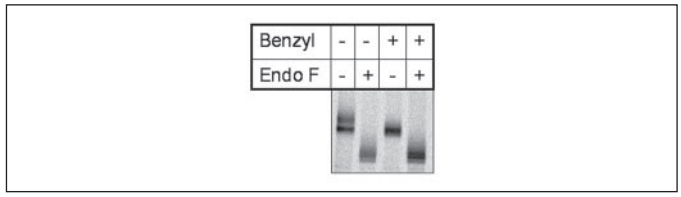

FIGURE 2. **PSMA is highly *N*- and *O*-glycosylated.** The transfection of COS-1 cells with hPSMA-pcDNA 3.1 was carried out either in the presence or in the absence of benzyl-GalNAc (denoted *Benzyl*) as inhibitor of the *O*-glycosylation process. After a 6-h pulse with [^{35}S]methionine, cells were harvested and PSMA was immunoprecipitated from the total cell lysate by J591 and 7E11 cells. The immunoprecipitates were divided into two aliquots and treated with Endo F or left untreated prior to SDS-PAGE analysis.

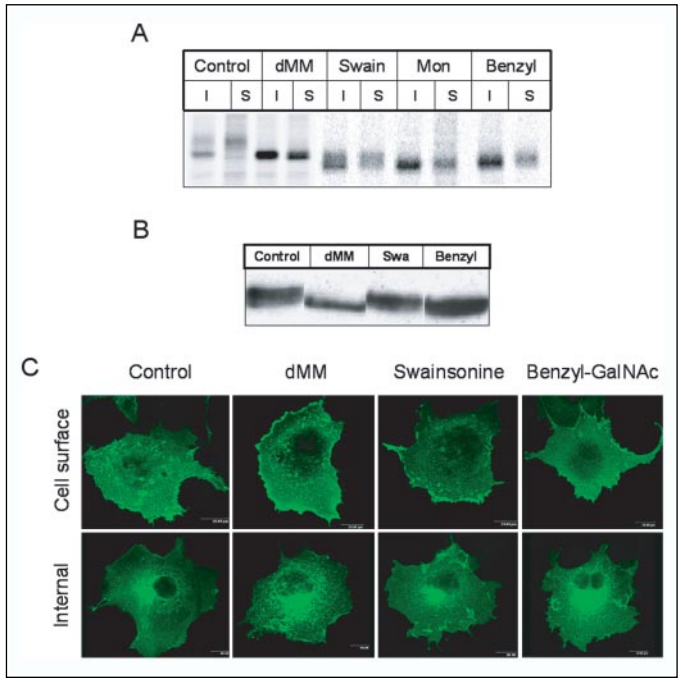

FIGURE 3. ***N*- and *O*-glycan modulation does not affect the cell-surface expression of PSMA.** *A*, cell-surface immunoprecipitation. Transiently transfected COS-1 cells were biosynthetically labeled with [^{35}S]methionine for 6 h in the presence or absence of modulators of *N*-glycosylation (dMM, swainsonine, and monensin) as well as *O*-glycosylation (benzyl-GalNAc). PSMA was immunoprecipitated from the cell surface (denoted *S*) and intracellular membranes (denoted *I*) using J591 mAb and a combination of J591 and 7E11c, respectively. The immunoprecipitates were finally analyzed by SDS-PAGE on 7% gels and subjected to a phosphorimaging device. The data presented here are the combination of two representative experiments. The very faint band appearing in the control sample (S fraction) of ~100 kDa is slightly smaller than the high-mannose form of PSMA and belongs to the background. *B*, cell-surface biotinylation. Transiently transfected COS-1 cells were treated for 48 h post-transfection with dMM, swainsonine, benzyl-GalNAc, or not treated and biotinylated with biotin-NHS. PSMA was immunoprecipitated from the total protein extracts and analyzed by Western blot using a peroxidase-conjugated streptavidin to detect the cell-surface-expressed PSMA molecules. *C*, cell-surface and intracellular localization of PSMA in the presence or absence of glycosylation inhibitors. Transfection and treatment of cells with inhibitors was as described in *B*. The cells were fixed with paraformaldehyde, permeabilized with saponin for cell-surface and intracellular localization (*lower panel*, internal) or not permeabilized for cell-surface detection (*upper panel*, cell surface). The cells were processed for indirect immunofluorescence using anti-PSMA (J591/7E11c) as the primary and Alexa Fluor 488-conjugated rabbit anti-mouse IgG as the secondary antibody. The images were analyzed using a Leica TCS SP2 confocal laser microscope.

human cancers and many glycosyl-epitopes constitute tumor-associated antigens (25). It is still unclear whether altered glycosylation in tumors affects the trafficking and therefore the exposure of tumor-associated antigens at the cell surface. We wanted therefore to investigate the glycosylation pattern of PSMA and its possible implication in the targeting and sorting of the protein.

Treatment of PSMA with Endo F, which cleaves both mannose-rich as well as complex glycans, has resulted in a drastic shift in the apparent molecular weight of PSMA concomitant with a high level of *N*-linked glycosylation of the protein (Fig. 2). The diffuse heterogeneous pattern of the protein band after Endo F treatment is most likely due to the sialylation of Endo F-resistant *O*-glycans. This type of glycosylation was examined by utilizing the sugar analogue benzyl-GalNAc in biosynthetic labeling experiments of transfected COS-1 cells. Benzyl-GalNAc strongly interferes with the *O*-glycosylation events by competing with GalNAc (26) and has been frequently used to examine the presence of *O*-glycan units in glycoproteins (27, 28). Fig. 2 demonstrates that benzyl-GalNAc treatment resulted in a significant reduction in the size of PSMA indicative of the existence of *O*-glycans in PSMA.

To investigate whether the extensive *N*- and *O*-glycosylation of PSMA may modulate intracellular transport and delivery of PSMA to the cell surface, we utilized a panel of inhibitors of *N*- and *O*-glycosylation in combination with cell-surface immunoprecipitation experiments. The J591 mAb was used to immunoprecipitate PSMA from intact cells, whereas a combination of J591 and 7E11c precipitated PSMA retained in the intracellular compartments from total cell lysates (Fig. 3*A*). *N*-Glycosylation was affected by incubating transfected COS-1 cells during biosynthesis with dMM, swainsonine, and monensin, all of which are reagents acting at different sites in the Golgi apparatus. Qualitative differences in the electrophoretic mobility of PSMA were obtained in the presence of these inhibitors compatible with altered carbohydrate patterns. Nevertheless, the modified glycoforms of PSMA reached the cell surface as the fully glycosylated PSMA indicating that modification of *N*-glycosylation is most likely not implicated in the transport of PSMA to the surface of COS-1 cells (Fig. 3*A*). A possible role of *O*-glycans was analyzed by using benzyl-GalNAc. Here again, the modified protein reached the cell surface as its control counterpart suggesting that also *O*-glycans do not influence the trafficking of PSMA.

We corroborated these data by employing cell-surface biotinylation followed by Western blot detection of PSMA glycoforms. As shown in Fig. 3*B* the modified forms of PSMA were detected at the cell surface and in almost similar amounts supporting the previous biosynthetic data.

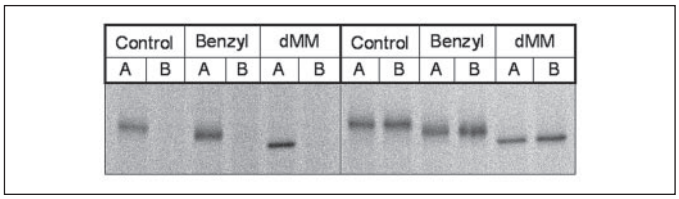

FIGURE 4. **Apical sorting of PSMA in polarized MDCK cells is not impaired by affecting *N*- and *O*-glycosylation.** PSMA was immunoprecipitated with the J591 mAb from apical (*A*) and basolateral (*B*) membranes of stably transfected MDCK cells grown on transmembrane filters. The possible effect of sugar moieties on the PSMA surface distribution was evaluated by incubating the cells with either benzyl-GalNAc (4 mM) or dMM (5 mM). Surface-expressed PSMA molecules are shown in the *left panel*, whereas the *right panel* shows PSMA immunoprecipitated from total cell lysates of both A- and B-fractions.

Finally we investigated the cell-surface and intracellular distribution of PSMA in the presence or absence of the glycosidase modulators using indirect immunofluorescence. In non-permeabilized transfected cells PSMA was found at the cell surface (Fig. 3*C*, *upper panel*). There was no significant difference in the images obtained in the presence or absence of the inhibitors dMM, swainsonine, or benzyl-GalNAc, providing additional support to the notion that modified glycoforms of PSMA are also transported to the cell surface. The intracellular localization of PSMA was also analyzed in saponin-permeabilized cells (Fig. 3*C*, *lower panel*). Here, the cell surface as well as Golgi membranes, and ER reticular networks were labeled supporting the biosynthetic pulse-chase data and the constitutive trafficking pathway of PSMA.

Sorting of PSMA in Stably Transfected MDCK Cells—For some glycoproteins *N*- and *O*-glycans have been proposed to act as signals for apical targeting in polarized cells (27, 29, 30). Predominant apical transport of PSMA has been recently demonstrated (31) in MDCK cells. Here, we address the question of whether impairment of *N*-glycosylation or prevention of *O*-glycosylation can cause a missorting of PSMA.

Fig. 4 illustrates the results of cell-surface immunoprecipitation of PSMA from the apical (*A*) and basolateral (*B*) membranes of an MDCK cell line stably transfected with PSMA. PSMA was predominantly found at the apical membrane (*left panel*). The basolateral membrane was almost devoid of PSMA, whereas the corresponding cellular lysates contained the protein (*right panel*). In the presence of the *O*-glycan inhibitor, benzyl-GalNAc, a reduction in the size of PSMA occurs, but no alteration in the cell-surface expression of PSMA was observed. Similarly, dMM, used here as a modulator of *N*-linked glycosylation, did not affect either the sorting profile or the modified PSMA glycoform. Together, the results indicate that processing of *N*- and *O*-glycosylation in the Golgi apparatus has no marked effect on the sorting of PSMA.

Folding of PSMA—Overexpression of PSMA in prostate cancer could generate aberrantly folded PSMA molecules that escape the quality control machinery in the ER (32). We wanted therefore to analyze the folding events of PSMA along its route to the cell surface in an overexpression cell system such as COS-1 cells and in MDCK cells, in which low copy of the PSMA gene is expressed.

We first studied a possible association of overexpressed PSMA in COS-1 cells with the ER-resident proteins BiP and calnexin. In a pulse-chase analysis (Fig. 5*A*), PSMA did not co-immunoprecipitate with BiP, whereas it was detected in the fractions that were immunodepleted from BiP. A very weak association with calnexin, a lectin-like membrane-bound chaperone of the ER, was found (Fig. 5*B*). The band corresponding to immature PSMA was discerned when a temperature block at 15 °C for 4 h was performed, which facilitated the accumulation of newly synthesized proteins in the ER. The binding to BiP and calnexin was also probed by Western blotting (Fig. 5*C*). Here, PSMA was immunoprecipitated from total cell lysates containing all forms of PSMA at steady state, and the immunoprecipitates were

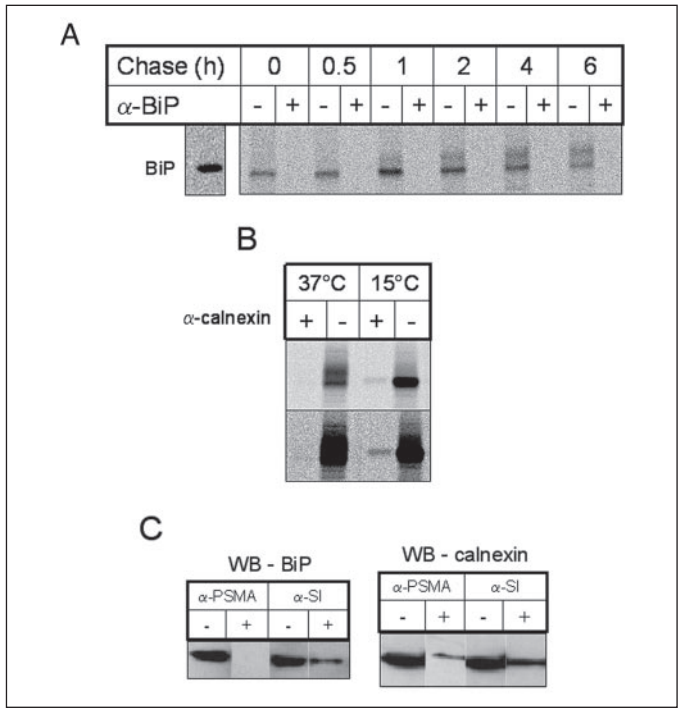

FIGURE 5. **PSMA does not associate with BiP and associates weakly with calnexin.** *A*, transfected COS-1 cells expressing PSMA were pulse-labeled with [^{35}S]methionine for 30 min and chased for the indicated time intervals. The detergent extracts were immunoprecipitated with anti-BiP antibodies, the antigenic material was eluted, and a combination of J591 and 7E11c was added to assess the presence of PSMA in the eluates (denoted '+'). The BiP-depleted samples were immunoprecipitated with anti-PSMA (denoted '−'). *B*, transfected cells were biosynthetically labeled for 4 h at 37 °C or pulse labeled for 1 h at 37 °C and chased for 4 h at 15 °C to generate an ER/ER/Golgi intermediate compartment block. The cellular extracts were immunoprecipitated with anti-calnexin antibodies, and the bound material was eluted and subjected to anti-PSMA mAb. The co-immunoprecipitating PSMA band was very faint. A better visualization of this band was achieved by intensifying the signal levels of the whole protein bands in the gel (*lower panel*). *C*, anti-PSMA antibodies were utilized in co-immunoprecipitation experiments to immunoprecipitate PSMA and possibly interacting BiP and calnexin. These two chaperones were detected by Western blotting (*WB*). As positive control the brush-border protein sucrase-isomaltase (*SI*) was used.

blotted with anti-BiP (Fig. 5*C*, *left*) or anti-calnexin antibodies (Fig. 5*C*, *right*). Here again, PSMA did not associate with BiP and calnexin bound weakly to the protein. Sucrase-isomaltase (and also lactase phlorizin hydrolase, data not shown), whose interaction with both BiP and calnexin was previously investigated (22, 33), were used here as positive controls. The binding of sucrase-isomaltase to both proteins was manyfold stronger than that of PSMA. BiP is therefore not directly involved in the folding events of PSMA. The weak binding of PSMA to calnexin strongly suggests that it occurs transiently for a short time before the third glucose is trimmed in the ER (34) and proposes that PSMA does not enter into consecutive glucosylation and deglucosylation cycles until it has acquired correct folding.

The next step was to examine the folding of PSMA and the time point of attainment of PSMA to a correct folding. We analyzed this issue by evaluating the sensitivity or resistance of PSMA toward proteases during intracellular trafficking. Here, two different proteases with distinct specificities were tested. Fig. 6*A* shows a representative experiment performed by treating the immunoprecipitated proteins with trypsin and chymotrypsin. Strikingly, PSMA was found either resistant or completely degraded by trypsin without producing a defined pattern of smaller fragments upon enzymatic digestion. Comparison between treated and non-treated samples showed that the mannose-rich form of PSMA is fully sensitive to trypsin, whereas the complex glycosylated PSMA acquires a substantial resistance toward the protease. An almost similar pattern was revealed by chymotrypsin. The complete sensitivity

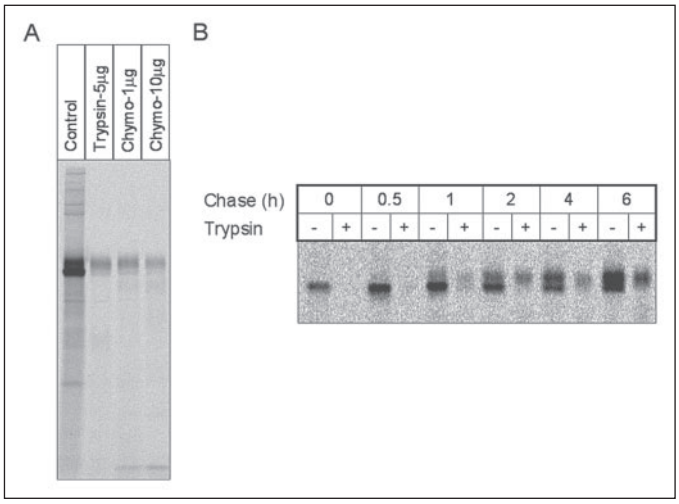

FIGURE 6. **The mannose-rich form of PSMA is highly sensitive to treatment with proteases.** *A*, immunoprecipitated PSMA was incubated 30 min at 37 °C in the presence of trypsin (5 μg) and chymotrypsin (1 and 10 μg). *B*, transfected COS-1 cells were labeled for 30 min with [^{35}S]methionine, washed, and chased for the indicated time intervals. Immunoprecipitation was performed with the J591 and 7E11c mAb, and the samples were divided into two equal parts and incubated for 30 min at 37 °C with (+) or without (−) 5 μg of trypsin in the presence of 10 μg of bovine serum albumin as a carrier protein.

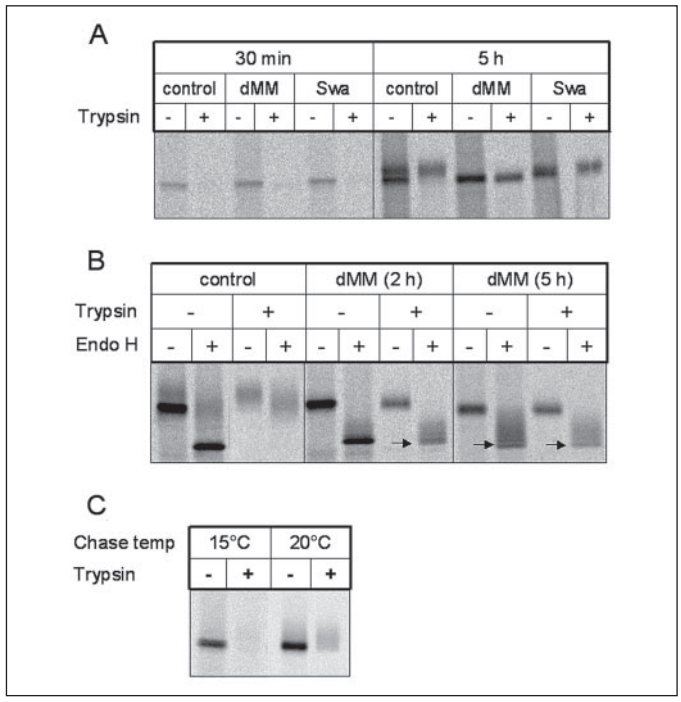

FIGURE 7. **Mannose-rich and other glycoforms of PSMA acquire resistance to trypsin in the Golgi apparatus.** *A*, transfected COS-1 cells were biosynthetically labeled with [^{35}S]methionine for 30 min or 5 h in the presence or absence of dMM (5 mM) and swainsonine (4 μg/μl), and the detergent extracts were immunoprecipitated with anti-PSMA mAb. The immunoprecipitates were digested with trypsin (5 μg) and analyzed by SDS-PAGE. *B*, transfected cells were biosynthetically labeled for 2 or 5 h in the presence or absence of dMM and treated or non-treated with trypsin followed by Endo H. The samples were finally analyzed by SDS-PAGE. *C*, transfected cells were labeled biosynthetically at 15 °C (for ER/ER/Golgi intermediate compartment block) and 20 °C (for Golgi block). PSMA was immunoprecipitated and treated with trypsin and the samples were finally subjected to SDS-PAGE.

of mannose-rich PSMA to trypsin did not change in pulse-chase experiments (Fig. 6*B*) strongly suggesting that no conformational alteration in mannose-rich glycosylated PSMA has occurred. In MDCK cells similar results were obtained indicating that overexpression of PSMA in COS-1 cells has no relevance to the acquisition of malfolded conformation by PSMA molecules in the ER (data are not shown). The trypsin sensitivity pattern of PSMA is unique to this protein, because its mannose-rich form never acquires trypsin resistance during its life cycle as other many other membrane proteins (for example see Refs. 35, 22, 29, and 36).

The complete sensitivity of mannose-rich PSMA and the resistance of its mature form toward trypsin led us to ask whether these differences are glycosylation-dependent or are rather the consequence of altered folding determinants that occur during intracellular transport after ER exit. To address this question, the pattern of *N*-glycosylation was modulated by labeling transfected COS-1 cells in the presence of dMM or swainsonine that inhibit processing of the PSMA chains in the *cis*- and medial Golgi, respectively. Cells were pulsed for 30 min (Fig. 7*A*, *left panel*) to visualize only the mannose-rich form of PSMA in the ER, or for 5 h (Fig. 7*A*, *right panel*) to detect also further processed PSMA forms. All the mannose-rich forms obtained in the presence or absence of the inhibitors after 30 min of pulse labeling were completely degraded with trypsin confirming the sensitivity of this form to the protease. After 5 h of labeling in the presence of swainsonine the modified glycoforms acquire trypsin-resistance comparable to the non-treated counterpart. Here again, the mannose-rich form remained trypsin-sensitive and was degraded as observed before. In the presence of dMM an Endo H-sensitive protein of a similar apparent molecular weight as its non-treated mannose-rich counterpart was the predominant glycoform of PSMA (Fig. 7*B*). dMM inhibits the function of α-mannosidase I in the *cis*-Golgi (37) and a mannose-rich-like species is the predominant form along the secretory pathway as has been observed for many proteins (38, 39). It should be noted that this mannose-rich form of PSMA is slightly different from that obtained in the absence of dMM, because it shows a faint smear upon Endo H treatment, due to partial processing of the mannose-rich PSMA. In the first 30 min of chase the dMM-treated PSMA was entirely sensitive to trypsin as shown for the non-treated protein. By contrast, 2 h into the chase at which time PSMA has arrived in the Golgi the Endo H-sensitive mannose-rich form was retained but has nevertheless acquired a substantial trypsin resistance. Strikingly, the trypsin resistance increases with chase times from 2 to 5 h (from 15% to 60% approximately). Obviously, the acquired resistance of complex glycosylated PSMA to trypsin is not due to the type of glycosylation *per se*, otherwise the dMM-treated mannose-rich PSMA would have been also degraded. It is rather the folding pattern of PSMA that dictates its sensitivity or susceptibility to the protease. As such the acquired resistance of the dMM mannose-rich PSMA to trypsin at 2 or 5 h of chase is solely due to correct folding of the protein that should be localized in the Golgi. This is supported by the observation that the half-life of the mannose-rich PSMA form is ~2 h, at which time the protein should have traversed the ER to the Golgi (see pulse-chase data above in Fig. 1). To further substantiate these data we performed a 20 °C temperature block to retain and accumulate PSMA molecules in the Golgi followed by examining their trypsin sensitivity. PSMA was visualized as a diffuse band that possibly comprises multiple processed glycoforms of the protein. Treatment of this protein form with trypsin revealed a similar type of band indicating an acquisition of correct trypsin-resistant conformation (Fig. 7*C*). On the contrary, molecules that were retained in the ER were again completely degraded. Altogether, the data unequivocally demonstrate that the mannose-rich ER form of PSMA does not acquire trypsin resistance at any time along its biosynthetic pathway.

We further assessed the folding of PSMA by utilizing the 7E11c antibody. Fig. 8 shows that the mAb 7E11c immunoprecipitates almost exclusively the mannose-rich form of PSMA under native conditions from TX-100 extracts of cells that were biosynthetically labeled for 5 h. For comparison, the J591 antibody has a wider specificity and reacts strongly with both

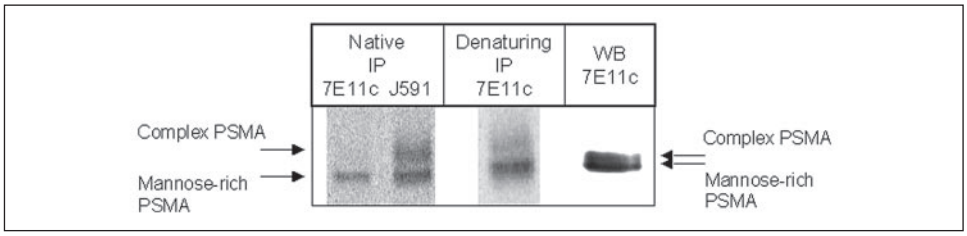

FIGURE 8. **Discrimination of the PSMA biosynthetic forms by the 7E11c antibody.** Transfected cells were labeled with [^{35}S]methionine for 5 h or not labeled. PSMA was immunoprecipitated under native condition from detergent extracts of the labeled cells with either mAb 7E11c or J591 (indicated native immunoprecipitation (*IP*)). Immunoprecipitation with denatured cell lysates was carried out with the 7E11c antibody (*Denaturing IP*). Non-labeled cells were immunoprecipitated with a combination of both antibodies and analyzed by Western blot using the 7E11c antibody (*WB*). Western blotting was performed using small slab gels.

biosynthetic forms of PSMA, the mannose-rich as well as the complex glycosylated species. On the other hand, Western blot analysis of PSMA using mAb 7E11c clearly demonstrates that this antibody has reacted not only with the mannose-rich form but also with the complex glycosylated PSMA protein (*right panel*). Likewise, when denatured lysates from 5-h biosynthetically labeled cells were immunoprecipitated with the 7E11c antibody an appreciable amount of the complex glycosylated PSMA then became detectable (*middle panel*). The 7E11c antibody is capable therefore of discriminating between differently folded forms of complex glycosylated PSMA, whereas it reacted with the mannose-rich form under native as well as denaturing conditions. This result is in line with the observations above that the folding of the complex glycosylated PSMA differs from that of the mannose-rich protein and that gross alterations in the folding of this latter form do not occur.

DISCUSSION

Understanding the molecular mechanisms underlying the biosynthesis, folding, intracellular transport, and polarized sorting of the type II membrane glycoprotein PSMA are essential and crucial prerequisites for its utilization as a therapeutically suitable target in prostate cancer. One interesting feature in the biosynthetic features of PSMA is the presence of high proportions of PSMA in an early immature mannose-rich glycosylated polypeptide through out its life cycle and also the slow transport rate between the ER and the Golgi. At first glance these characteristics suggest that PSMA is retained for a prolonged time in the ER where it associates with members of the quality control machinery, such as BiP and calnexin, until it has acquired a correct conformation and transport competence before ER egress.

Strikingly, however, a conformational maturation of mannose-rich PSMA does not occur as evidenced by protease sensitivity tests and antibody binding. Remarkably, the initial mannose-rich biosynthetic form of PSMA is readily degraded with trypsin (or chymotrypsin) and does not acquire a different proteolytic pattern throughout its entire biosynthetic life cycle. This strongly suggests that no gross conformational alterations have occurred in mannose-rich PSMA. By contrast, complex glycosylated PSMA is predominantly resistant to the proteases indicative of acquisition of a correct folding or of a protective function of the complex oligosaccharides. Nevertheless, this latter possibility could be excluded, because modulation and inhibition of complex glycosylation of PSMA in the Golgi, for example, by dMM or swainsonine results in equally trypsin-resistant glycoforms. This finding is surprising for an endogenous protein in view of current knowledge of protein anterograde transport and the consensus that proteins fold and acquire transport-competent conformation in the ER before leaving this organelle (40). Also the binding patterns of early biosynthetic PSMA forms to typical ER chaperones, such as BiP and calnexin, do not conform to well known concepts of quality control mechanism in the ER (41). Although BiP does not associate with PSMA at all, calnexin does albeit to a very low extent, suggesting that it does not enter into a glucosylation and deglucosylation calnexin cycles (42). An implication of other chaperones, such as ERp57 (43), in an early binding to PSMA cannot be completely excluded. A role of the ER and its chaperones in the folding of PSMA, however, is not favored, because an alteration in the folding pattern of the initial mannose-rich PSMA conformation does not occur.

It is possible that the trypsin-sensitive state of PSMA is subject to a secondary quality control that operates beyond the ER. In a few cases of mutant membrane and secretory proteins this mechanism has been proposed, because these mutants do not acquire correct folding and yet are able to exit the ER and reside in the ER/Golgi intermediate compartment and Golgi compartments (33, 44, 45, 46). More recently, a phenylalanine-based signal in sucrase-isomaltase has been identified to specify Golgi retention (47) strongly proposing the existence of signal-recognition partners that contribute to a post-ER control mechanism.

In this report we unequivocally demonstrate that PSMA is not only an extensively *N*-glycosylated, but also a heavily *O*-glycosylated, membrane glycoprotein. PSMA has not been described before to carry *O*-glycans. As such this finding is of particular interest in view of the crucial role played by *O*-glycosidically linked carbohydrate chains on the cell surfaces of cancer cells (for a review see Ref. 48) and the role of PSMA as a potential target in prostate cancer cells. In cancerous cells, the structures of *O*-glycans on membrane glycoproteins are often unusual or abnormal and greatly contribute to the phenotype and biology of cancer cells. This is borne out by the fact that glycosyltransferases and sulfotransferases that are implicated in the synthesis of *O*-glycans are regulated in a tissue- and growth-specific fashion.

In view of the observations that proper folding occurs in the Golgi it was essential to examine the transport behavior of PSMA as a function of *O*-glycosylation and also other glycans modifications in the Golgi. Our data show that *O*-glycans do not affect the cell-surface expression of PSMA, because their modulation with the potent *O*-glycosylation inhibitor, benzyl-GalNAc, generates a marked size shift, nevertheless the PSMA glycoform is transported to the cell surface as its non-treated counterpart. Similarly, *N*-glycans appear not to affect the transport and cell-surface expression of PSMA. Inhibitors of *N*-glycan processing in the Golgi, dMM, swainsonine, or monensin (49) generate qualitatively altered PSMA glycoforms, but the transport of these glycoforms to the cell surface remains virtually similar to that of non-treated PSMA. Also inhibition of glucose trimming in the ER by dNM has no effects on the localization of PSMA at the cell surface (data not shown). Entire blocking of cotranslational *N*-glycosylation, for example by using tunicamycin, and assessment of its resulting effect is completely avoided in our studies, because this may associate with malfolding and aggregation of PSMA as shown for many other proteins. Along this, a possible retarded or inhibited targeting of PSMA (16, 50) may be interpreted either as being due to an aggregated and malfolded PSMA conformation or *N*-glycosylation is indeed responsible for the observed effect. On the

other hand, generation of single substitution mutants of potential *N*-glycosylation sites in the ectodomain of PSMA have no influence on the transport of PSMA (16) supporting thus the notion that *N*-glycosylation is not implicated in the trafficking of the molecule.

Although these conclusions are obvious in the non-polarized COS-1 cells, an involvement of *N*- or *O*-glycans in the polarized sorting of PSMA, which is normally expressed in polar epithelial cells, cannot be excluded. An assessment of a putative role of glycosylation on PSMA trafficking is particularly important in view of current knowledge in which the sorting of apical proteins has been shown to be directly linked to an intact *O*-glycosylation (51) or *N*- and *O*-glycosylation patterns (29, 52). In MDCK cells, a prototype of epithelial cells, PSMA is transported with high fidelity and localized exclusively to the apical membrane. Analysis of the role of *O*- and *N*-glycans in these cells reveals that neither one of the glycosylation types alters the efficient apical sorting pattern of PSMA. For many proteins the structural and functional stability as well as the transport competence and targeting fidelity strongly rely on an efficiently processed and correctly synthesized *N*- and *O*-glycans (27, 53). As our results unequivocally demonstrate, it is obvious that glycosylation does not constitute a structural element in the context of a putative sorting signal of PSMA, and we strongly propose the existence of a proteinaceous signal type.

Of particular interest in the sorting mechanism of PSMA is the presence of a di-leucine-based motif at the N-terminal cytoplasmatic tail of the protein. In many proteins di-leucine motifs constitute an efficient targeting signal to the basolateral membrane (54, 55). In the context of PSMA, however, this putative signal is either non-functional in PSMA, or more likely, the exclusive apical sorting of PSMA suggests that the strong apical sorting signal of PSMA is dominant over the di-leucine motif. The latter possibility is in line with a growing body of knowledge that has established that apical sorting mechanisms are mediated by specific sorting signals and these are in many cases more efficient than and dominant over basolateral signals (56, 57). The ability of PSMA to acquire a correctly folded state in the Golgi and to be efficiently transported and targeted correctly to the apical membrane, regardless of its glycosylation state, is an essential asset in using this protein as a therapeutic target in metastasizing cells in which glycosylation patterns differ at various stages of tumor progression.

Acknowledgements—We thank Drs. Hans-Peter Hauri, Biocenter Basel, and Erwin Sterchi, University of Bern, Switzerland for the gift of antibodies against sucrase-isomaltase.

REFERENCES

1. Landers, K. A., Burger, M. J., Tebay, M. A., Purdie, D. M., Scells, B., Samaratunga, H., Lavin, M. F., and Gardiner, R. A. (2005) *Int. J. Cancer* **114,** 950–956
2. Gong, M. C., Chang, S. S., Sadelain, M., Bander, N. H., and Heston, W. D. (1999) *Cancer Metastasis Rev.* **18,** 483–490
3. Horoszewicz, J. S., Kawinski, E., and Murphy, G. P. (1987) *Anticancer Res.* **7,** 927–935
4. Israeli, R. S., Powell, C. T., Fair, W. R., and Heston, W. D. (1993) *Cancer Res.* **53,** 227–230
5. Israeli, R. S., Powell, C. T., Corr, J. G., Fair, W. R., and Heston, W. D. (1994) *Cancer Res.* **54,** 1807–1811
6. Pangalos, M. N., Neefs, J. M., Somers, M., Verhasselt, P., Bekkers, M., van der, H. L., Fraiponts, E., Ashton, D., and Gordon, R. D. (1999) *J. Biol. Chem.* **274,** 8470–8483
7. Luthi-Carter, R., Barczak, A. K., Speno, H., and Coyle, J. T. (1998) *J. Pharmacol. Exp. Ther.* **286,** 1020–1025
8. Troyer, J. K., Beckett, M. L., and Wright, G. L., Jr. (1995) *Int. J. Cancer* **62,** 552–558
9. Murphy, G. P., Kenny, G. M., Ragde, H., Wolfert, R. L., Boynton, A. L., Holmes, E. H., Misrock, S. L., Bartsch, G., Klocker, H., Pointner, J., Reissigl, A., McLeod, D. G., Douglas, T., Morgan, T., and Gilbaugh, J., Jr. (1998) *Urology* **51,** 89–97
10. Chang, S. S., Reuter, V. E., Heston, W. D., Bander, N. H., Grauer, L. S., and Gaudin, P. B. (1999) *Cancer Res.* **59,** 3192–3198
11. Babaian, R. J., Sayer, J., Podoloff, D. A., Steelhammer, L. C., Bhadkamkar, V. A., and Gulfo, J. V. (1994) *J. Urol.* **152,** 1952–1955
12. Liu, H., Rajasekaran, A. K., Moy, P., Xia, Y., Kim, S., Navarro, V., Rahmati, R., and Bander, N. H. (1998) *Cancer Res.* **58,** 4055–4060
13. Jansen, F. K., Blythman, H. E., Carriere, D., Casellas, P., Gros, O., Gros, P., Laurent, J. C., Paolucci, F., Pau, B., Poncelet, P., Richer, G., Vidal, H., and Voisin, G. A. (1982) *Immunol. Rev.* **62,** 185–216
14. Fracasso, G., Bellisola, G., Cingarlini, S., Castelletti, D., Prayer-Galetti, T., Pagano, F., Tridente, G., and Colombatti, M. (2002) *Prostate* **53,** 9–23
15. Holmes, E. H., Greene, T. G., Tino, W. T., Boynton, A. L., Aldape, H. C., Misrock, S. L., and Murphy, G. P. (1996) *Prostate Suppl.* **7,** 25–29
16. Barinka, C., Sacha, P., Sklenar, J., Man, P., Bezouska, K., Slusher, B. S., and Konvalinka, J. (2004) *Protein Sci.* **13,** 1627–1635
17. Ghosh, A., and Heston, W. D. (2003) *Prostate* **57,** 140–151
18. Schulke, N., Varlamova, O. A., Donovan, G. P., Ma, D., Gardner, J. P., Morrissey, D. M., Arrigale, R. R., Zhan, C., Chodera, A. J., Surowitz, K. G., Maddon, P. J., Heston, W. D., and Olson, W. C. (2003) *Proc. Natl. Acad. Sci. U. S. A.* **100,** 12590–12595
19. Naim, H. Y., Lacey, S. W., Sambrook, J. F., and Gething, M. J. (1991) *J. Biol. Chem.* **266,** 12313–12320
20. Jacob, R., Weiner, J. R., Stadge, S., and Naim, H. Y. (2000) *J. Biol. Chem.* **275,** 10630–10637
21. Naim, H. Y., Sterchi, E. E., and Lentze, M. J. (1987) *Biochem. J.* **241,** 427–434
22. Jacob, R., Bulleid, N. J., and Naim, H. Y. (1995) *J. Biol. Chem.* **270,** 18678–18684
23. Ouwendijk, J., Moolenaar, C. E., Peters, W. J., Hollenberg, C. P., Ginsel, L. A., Fransen, J. A., and Naim, H. Y. (1996) *J. Clin. Invest.* **97,** 633–641
24. Jacob, R., Alfalah, M., Grunberg, J., Obendorf, M., and Naim, H. Y. (2000) *J. Biol. Chem.* **275,** 6566–6572
25. Hakomori, S. (2002) *Proc. Natl. Acad. Sci. U. S. A.* **99,** 10231–10233
26. Kojima, N., Handa, K., Newman, W., and Hakomori, S. (1992) *Biochem. Biophys. Res. Commun.* **182,** 1288–1295
27. Alfalah, M., Jacob, R., Preuss, U., Zimmer, K. P., Naim, H., and Naim, H. Y. (1999) *Curr. Biol.* **9,** 593–596
28. Huet, G., Gouyer, V., Delacour, D., Richet, C., Zanetta, J. P., Delannoy, P., and Degand, P. (2003) *Biochimie* (*Paris*) **85,** 323–330
29. Alfalah, M., Jacob, R., and Naim, H. Y. (2002) *J. Biol. Chem.* **277,** 10683–10690
30. Yeaman, C., Le Gall, A. H., Baldwin, A. N., Monlauzeur, L., Le Bivic, A., and Rodriguez-Boulan, E. (1997) *J. Cell Biol.* **139,** 929–940
31. Christiansen, J. J., Rajasekaran, S. A., Moy, P., Butch, A., Goodglick, L., Gu, Z., Reiter, R. E., Bander, N. H., and Rajasekaran, A. K. (2003) *Prostate* **55,** 9–19
32. Stefani, M. (2004) *Biochim. Biophys. Acta* **1739,** 5–25
33. Propsting, M. J., Jacob, R., and Naim, H. Y. (2003) *J. Biol. Chem.* **278,** 16310–16314
34. Abeijon, C., and Hirschberg, C. B. (1992) *Trends Biochem. Sci.* **17,** 32–36
35. Fransen, J. A., Hauri, H. P., Ginsel, L. A., and Naim, H. Y. (1991) *J. Cell Biol.* **115,** 45–57
36. Naim, H. Y. (1992) *Biochem. J.* **286,** 451–457
37. Fuhrmann, U., Bause, E., Legler, G., and Ploegh, H. (1984) *Nature* **307,** 755–758
38. Naim, H. Y., Joberty, G., Alfalah, M., and Jacob, R. (1999) *J. Biol. Chem.* **274,** 17961–17967
39. Muto, S., Takada, T., and Matsumoto, K. (2001) *Biochim. Biophys. Acta* **1527,** 39–46
40. Lee, M. C., Miller, E. A., Goldberg, J., Orci, L., and Schekman, R. (2004) *Annu. Rev. Cell Dev. Biol.* **20,** 87–123
41. High, S., Lecomte, F. J., Russell, S. J., Abell, B. M., and Oliver, J. D. (2000) *FEBS Lett.* **476,** 38–41
42. Taylor, S. C., Thibault, P., Tessier, D. C., Bergeron, J. J., and Thomas, D. Y. (2003) *EMBO Rep.* **4,** 405–411
43. Oliver, J. D., van der Wal, F. J., Bulleid, N. J., and High, S. (1997) *Science* **275,** 86–88
44. Hammond, C., and Helenius, A. (1994) *J. Cell Biol.* **126,** 41–52
45. Moolenaar, C. E., Ouwendijk, J., Wittpoth, M., Wisselaar, H. A., Hauri, H. P., Ginsel, L. A., Naim, H. Y., and Fransen, J. A. (1997) *J. Cell Sci.* **110,** 557–567
46. Ito, M., Amizuka, N., Ozawa, H., and Oda, K. (2002) *Biochem. J.* **361,** 473–480
47. Propsting, M. J., Kanapin, H., Jacob, R., and Naim, H. Y. (2005) *J. Cell Sci.* **118,** 2775–2784
48. Brockhausen, I. (1999) *Biochim. Biophys. Acta* **1473,** 67–95
49. Marchal, I., Mir, A. M., Kmiecik, D., Verbert, A., and Cacan, R. (1999) *Glycobiology* **9,** 645–654
50. Tkacz, J. S., and Lampen, O. (1975) *Biochem. Biophys. Res. Commun.* **65,** 248–257
51. Spodsberg, N., Alfalah, M., and Naim, H. Y. (2001) *J. Biol. Chem.* **276,** 46597–46604
52. Pang, S., Urquhart, P., and Hooper, N. M. (2004) *J. Cell Sci.* **117,** 5079–5086
53. Scheiffele, P., Peranen, J., and Simons, K. (1995) *Nature* **378,** 96–98
54. Bello, V., Goding, J. W., Greengrass, V., Sali, A., Dubljevic, V., Lenoir, C., Trugnan, G., and Maurice, M. (2001) *Mol. Biol. Cell* **12,** 3004–3015
55. Miranda, K. C., Khromykh, T., Christy, P., Le, T. L., Gottardi, C. J., Yap, A. S., Stow, J. L., and Teasdale, R. D. (2001) *J. Biol. Chem.* **276,** 22565–22572
56. Jacob, R., Preuss, U., Panzer, P., Alfalah, M., Quack, S., Roth, M. G., Naim, H., and Naim, H. Y. (1999) *J. Biol. Chem.* **274,** 8061–8067
57. Vogel, L. K., Sahkri, S., Sjostrom, H., Noren, O., and Spiess, M. (2002) *J. Biol. Chem.* **277,** 13883–13888

Apical Transport and Folding of Prostate-specific Membrane Antigen Occurs Independent of Glycan Processing

Deborah Castelletti, Giulio Fracasso, Marwan Alfalah, Sara Cingarlini, Marco Colombatti and Hassan Y. Naim

J. Biol. Chem. 2006, 281:3505-3512.
doi: 10.1074/jbc.M509460200 originally published online October 12, 2005
